Published in final edited form as:
Nucl Med Biol. 2013 February ; 40(2): 245–251. doi:10.1016/j.nucmedbio.2012.10.010.

Comparison of two cross-bridged macrocyclicchelators for the evaluation of ^{64}Cu-labeled-LLP2A, a peptidomimetic ligand targeting VLA-4-positive tumors

Majiong Jiang[†,||], **Riccardo Ferdani**[‡], **Monica Shokeen**[‡], and **Carolyn J. Anderson**[†,‡,||,*]

[†]Department of Chemistry, Washington University, St. Louis, Missouri, USA

[‡]Mallinckrodt Institute of Radiology, Washington University, St. Louis, Missouri, USA

[||]Department of Radiology, University of Pittsburgh, Pittsburgh, Pennsylvania, USA

Abstract

Integrin $\alpha_4\beta_1$ (also called very late antigen-4 or VLA-4) plays an important role in tumor growth, angiogenesis and metastasis, and there has been increasing interest in targeting this receptor for cancer imaging and therapy. In this study, we conjugated a peptidomimetic ligand known to have good binding affinity for $\alpha_4\beta_1$ integrin to a cross-bridged macrocyclicchelator with a methane phosphonic acid pendant arm, CB-TE1A1P. CB-TE1A1P-LLP2A was labeled with ^{64}Cu under mild conditions in high specific activity, in contrast to conjugates based on the "gold standard" di-acid cross-bridged chelator, CB-TE2A, which require high temperatures for efficient radiolabeling. Saturation binding assays demonstrated that ^{64}Cu-CB-TE1A1P-LLP2A had comparable binding affinity(1.2 nM vs 1.6 nM) but more binding sites(B_{max} = 471 fmol/mg) in B16F10 melanoma tumor cells than ^{64}Cu-CB-TE2A-LLP2A (B_{max} = 304 fmol/mg, $p < 0.03$). In biodistribution studies, ^{64}Cu-CB-TE1A1P-LLP2A had less renal retention but higher uptake in tumor(11.4 ± 2.3 %ID/g versus 3.1± 0.6 %ID/g, $p<0.001$)and other receptor-rich tissues compared to ^{64}Cu-CB-TE2A-LLP2A. At 2 h post-injection, ^{64}Cu-CB-TE1A1P-LLP2A also had significantly higher tumor: blood and tumor: muscle ratios than ^{64}Cu-CB-TE2A-LLP2A(CB-TE1A1P = 19.5 ± 3.0 and 13.0 ± 1.4, respectively, CB-TE2A = 4.2 ± 1.4 and 5.5 ± 0.9, respectively, $p< 0.001$). These data demonstrate that ^{64}Cu-CB-TE1A1P-LLP2A is an excellent PET radiopharmaceutical for the imaging of $\alpha_4\beta_1$ positive tumors and also has potential for imaging other $\alpha_4\beta_1$ positive cells such as those of the pre-metastatic niche.

INTRODUCTION

Membrane receptors of the integrin family are well-characterized targets in cancer cells. As a family of adhesive proteins, integrins have been reported to mediate interactions between adhesion molecules on adjacent cells and/or the extracellular matrix (ECM) and are involved in biological processes including cell migration and metastasis.[1–2] Integrin $\alpha_4\beta_1$ (also called very late antigen-4 or VLA-4) is a heterodimeric transmembrane receptor that is widely expressed on a variety of tumors. There is increasing evidence that $\alpha_4\beta_1$ integrin plays an

[*]Corresponding Author: Carolyn J. Anderson, Ph.D., Department of Radiology, University of Pittsburgh, 100 Technology Drive, Suite 452, Pittsburgh, PA 15219, Phone: 412-624-6887, andersoncj@upmc.edu.

important role in tumor growth, angiogenesis and metastasis,[3–5] therefore $\alpha_4\beta_1$ integrin is a promising target for imaging and therapy of lymphoid malignancy cancers.

Radiolabeled receptor-targeted peptides have attracted attention for tumor diagnosis and therapy. This is primarily due to the ease of peptide synthesis, their favorable pharmacokinetic characteristics together with their flexibility in chemical modification and radiolabeling.[6–7] LLP2A, a peptidomimetic ligand that has high affinity for $\alpha_4\beta_1$ integrin, was first reported by Peng, *et al.* as identified from a highly focused one-bead-one-compound combinatorial library.[8] They demonstrated that LLP2A specifically targeted $\alpha_4\beta_1$-positive tumors in nude mouse xenografts with *in vivo* near infrared optical imaging.

LLP2A was also conjugated to 11-bis(carboxymethyl)-1,4,8,11-tetraaza-bicyclo[6.6.2] hexadecane (CB-TE2A), a highly stable ^{64}Cu chelator, as ^{64}Cu-CB-TE2A-LLP2A. In the Raji tumor-bearing mouse model, small-animal PET imaging demonstrated that ^{64}Cu-CB-TE2A-LLP2A accumulated in tumor and spleen, which are $\alpha_4\beta_1$ integrin-rich tissues.[9] In another study, Shokeen *et al.* showed that ^{64}Cu-CB-TE2A-LLP2A can image $\alpha_4\beta_1$ positive bone marrow-derived cells in sites of bone metastasis in a mouse model of metastatic breast cancer.[10]

Although ^{64}Cu-CB-TE2A bioconjugates show significant improvement over those with non-bridged macrocycles with respect to *in vivo* stability,[11] one of the disadvantages of CB-TE2A is the requirement of harsh conditions for radiolabeling with ^{64}Cu, typically 95 °C for 1–1.5 h.[12] To broaden the applications of the cross-bridged bifunctional chelator, a second generation chelator was developed by incorporating methanephosphonic acid pendant arms.[13] The substitution of methanephosphonic acid pendant arms brings higher selectivity for Cu(II) and a greater ease of ^{64}Cu incorporation, while retaining high kinetic stability. A mixed armed chelator, CB-TE1A1P(1,4,8,11-tetraazacyclotetradecane-1-(methanephosphonic acid)-8-(methanecarboxylic acid) was developed, featuring a methanephosphonic acid as well as a carboxymethyl pendant arm for conjugation to primary amines on peptides and proteins.[14] Radiolabeling of CB-TE1A1P showed that the ^{64}Cu complex can be formed at room temperature after 30 min, achieving a radiochemical yield of >95%. Here, we report radiochemistry as well as *in vitro* and *in vivo* characterization of ^{64}Cu-CB-TE1A1P-LLP2A and ^{64}Cu-CB-TE2A-LLP2A in the $\alpha_4\beta_1$-positive B16F10 tumor model.

MATERIALS AND METHODS

Copper-64 ($t_{1/2}$ = 12.7 hours, β^+; 17.8%, $E_{\beta+max}$ = 656 KeV, β^-, 38.4%, $E_{\beta-max}$ = 573 KeV) was obtained from Washington University (St. Louis, MO) and University of Wisconsin (Madison, WI). All chemicals were purchased from Sigma-Aldrich Chemical Co. (St. Louis, MO), unless otherwise specified. Aqueous solutions were prepared using ultrapure water (resistivity, 18 MΩ). Rink amide 4-methylbenzhydrylamine resin (loading, 0.77 mmol/g) and all Fmoc protected amino acid were purchased from Chem-Impex International, Inc. (Wood Dale, IL). CB-TE1A1P and CB-TE2A were prepared according to literature procedures.[14,15] Analytical and semi-preparative reversed-phase high-performance liquid chromatography (HPLC) were performed either on a Waters 600E (Milford, MA) chromatography system with a Waters 991 photodiode array detector and an Ortec model 661 (EG&G Instruments, Oak Ridge, TN) radioactivity detector, or a Waters 1525 Binary HPLC pump (Milford, MA) with a Waters 2489 UV/visible detector and a model 105-S-1(Carroll& Ramsey Associates; Berkeley, CA) radioactivity detector. Non-radioactive HPLC samples were analyzed on an analytical C18 column (Vydac, Deerfield, IL) and purified on a semi-preparative C18 column (Waters, Milford, MA). Radiochemistry reaction progress and purity were monitored on a rocket C18 column (Alltima, Deerfield, IL). The

mobile phase was H_2O (0.1% TFA; solvent A) and acetonitrile (0.1% TFA; solvent B). Radioactive samples were counted using an automated well-type gamma-counter (8000; Beckman, Irvine, CA). PET/CT data were acquired using either an Inveon Preclinical Imaging Station or a Focus 220 (Siemens Medical Solutions), and the CT images were acquired with an Inveon Preclinical Imaging Station.

Synthesis of CB-TE2A-LLP2A and CB-TE1A1P-LLP2A

CB-TE2A-LLP2A was prepared as previously described.[9] CB-TE1A1P-LLP2A was designed to have CB-TE1AP attached to the side chain of Lys and 2 hydrophilic linkers (N-(Fmoc-8-amino-3,6-dioxa-octyl)succinamic acid)between LLP2A and Lys(CB-TE1AP). Fmoc-Lys(Dde)-OH, followed by 2 linkers coupled to Lys (Dde), and then LLP2A were assembled on the N terminus of the linker as previously reported.[8] The Dde protecting group was removed by washing twice with 2% NH_2NH_2 in DMF (at 5 and 10 min), and the beads were washed again with DMF, MeOH, and DMF. The CB-TE1A1P.2TFA salt (62.5 mg, 165 μmol) was first dissolved in DMF. DIC (20.9 mg, 165 μmol) and DIEA (42.5 mg, 330 μmol) were added to this solution followed by stirring for 30 min before adding to the resin (66 μmol of LLP2A). The mixture was gently rotated overnight and filtered. The beads were thoroughly washed with DMF, MeOH, and DCM and then dried under vacuum for 1 h. Cleavage of compounds from the resin and removal of the protecting group were achieved simultaneously over 2 h at room temperature with a mixture of 95% TFA: 2.5% water: 2.5% triisopropylsilane. The crude product was precipitated with cold ether and purified by semi-preparative reversed-phase HPLC (10 ×250 mm, 10 μm; Waters) using two solvent systems with the gradient elution method at a flow rate of 3 mL/min. Solvent A was 0.1% TFA in water, and solvent B was 0.1% TFA in acetonitrile. The elution method started with a linear gradient from 90% to 80%A over 3 min, followed by 80% to 45% A over 16 min, and from 45% to 10% A over 3 min. The elution profile was monitored by UV absorbance at 254 nm. Purified CB-TE1A1P-LLP2A was a white powder after lyophilization in water/acetonitrile mixture. The compound was characterized by analytical HPLC and electrospray mass spectroscopy. The purity was determined to be greater than 97% while the overall yield was 25%. The identity of the compounds was confirmed by matrix-assisted laser desorption/ ionization time-of-flight mass spectrometry(MALDI-TOF-MS; MS [MH+]:1759.96; theoretical value: 1758.95).

Radiolabeling of CB-TE1A1P-LLP2A and CB-TE2A-LLP2A with ^{64}Cu

$^{64}CuCl_2$ (5–10 μL in 0.5 M HCl) was diluted with 0.1 M ammonium acetate buffer (pH 8, 50–100 μL). The CB-TE1A1P-LLP2A or CB-TE2A-LLP2A solution (1 μg) was mixed with ^{64}Cu-acetate (1 mCi) with a final volume of 100 μL in 0.1 M ammonium acetate buffer (pH=8.1). The mixture was incubated at 40, 60, 90 °C for 5–60 min. After incubation, the radiochemical purity (RCP) of the ^{64}Cu-labeled CB-TE1A1P-LLP2A was monitored by radio-HPLC with a rocket C18 column (7 × 53 mm, 3 μm; Alltima). The elution method used two solvent systems A (water/0.1% TFA) and B (acetonitrile/0.1% TFA) at a flow rate of 3 mL/min with the gradient protocols: 100% to 90% A over 3 min, followed by 90% to 10% A in 6 min.

Flow cytometry

A phycoerythrin-conjugated antibody to Mouse CD49d (Integrin alpha 4) was purchased from eBioscience (San Diego, CA). B16F10 cells were prepared for flow cytometry by incubating cells with monoclonal antibodies followed by phosphate-buffered saline (PBS) washes. Data collection and analyses were performed on a FACS Aria flow cytometer (BD Biosciences, San Jose, CA).

Saturation binding assay

All cell handling was aseptically performed in a laminar flow hood. The B16F10 melanoma cell line was purchased from the American Tissue Culture Collection (ATCC) and was grown until 60–75% confluent in T75 flasks. The cells were maintained at a concentration of 1×10^6 cells/mL in Iscove's modified Dulbeccos's medium (GIBCO-BRL) at 37°C in a humidified atmosphere with 5% CO_2 in a Revco Elite II incubator. To determine cell density, equal amounts of cell suspension and trypan blue exclusion were added to a hemocytometer to calculate a cells/mL concentration and ensure cell viability.

Cell experiments were performed to determine the binding affinity of ^{64}Cu-CB-TE1A1P-LLP2A and ^{64}Cu-CB-TE2A-LLP2A in VLA-4 positive B16F10 mouse melanoma cells. Cells were grown in Iscoves MDM until 60–75% confluent, harvested by mechanical dissociation and re-suspended in the in 24-well plates (200,000 cells per well) 24 h prior to the experiment. Before the experiment, cells were washed with 1 mL HBSS twice and 0.5 mL binding media (HBSS with 0.1% BSA and 1 mM Mn^{2+}) was added to each well. Then 12 μg of LLP2A was added to half of the wells as cold block to determine *in vitro* non-specific binding, followed by ^{64}Cu-CB-TE1A1P-LLP2A or ^{64}Cu-CB-TE2A-LLP2A in increasing concentrations (0.1–80 nM). The samples were incubated for 2 hon ice (4 °C). After incubation, the radioactive media was removed. Cell pellets were rinsed with ice cold binding buffer (1 mL) twice and dissolved in 0.5% SDS solution. The radioactivity in each fraction was measured in a well counter (Packard II gamma counter). The protein content of each cell lysate sample was determined (BCA Protein Assay Kit, Pierce). The measured radioactivity associated with the cells was normalized to the amount of cell protein present (cpm/mg protein).

Biodistribution studies in B16F10 tumor-bearing mice

All animal studies were performed under the *Guide for the Care and Use of Laboratory Animals* (11) under the auspices of the Washington University Animal Studies Committee. B16F10 melanoma cells in PBS were mixed 1:1 (v:v) with Matrigel Basement Membrane Matrix (Becton Dickinson, Franklin Lakes, NJ), and 200 μL (1×10^7 cells) were injected subcutaneously into 7-wk-old C57BL/6 mice (Charles River Laboratories). The tumors were allowed to grow for 14–21 d (619 ±261 mg), and the mice ($n = 5$ per group) were injected intravenously with 14 μCi (14 ng) of ^{64}Cu-CB-TE1A1P-LLP2A The tumor bearing mice were sacrificed at 2 h post-injection, and the blood, marrow, fat, heart, stomach, intestines, lungs, liver, spleen, kidneys, muscle, bone, pancreas, and tumor were harvested, weighed, and counted in a -counter. An additional group of mice was injected with ^{64}Cu-CB-TE1A1P-LLP2A premixed with 50 μg of LLP2A to serve as a blocking agent and sacrificed at 2 h. The percent injected dose per gram of tissue (%ID/g) was determined by decay correction of the ^{64}Cu-labeled LLP2A for each sample normalized to a standard of known weight, which was representative of the injected dose.

Small animal PET/CT images

Six mice were injected intravenously (tail vein) with ^{64}Cu-CB-TE1A1P-LLP2A(100 μCi, 667 ng)and six mice were injected intravenously with ^{64}Cu-CB-TE2A-LLP2A (100 μCi, 667 ng). Half of the mice received a dose that was premixed with 100 μg LLP2A serving as a blocking agent. At 2 and 24 h post injection, mice were anaesthetized with 1–2% isoflurane and small animal PET and CT imaging was performed. Static images were collected for 15 or 30 min and co-registered with Inveon Research Workstation software (Siemens Medical Solutions, Knoxville, TN). PET images were re-constructed with the maximum *a posteriori* (MAP) algorithm. The analysis of the small animal PET images was done using ASIPro software, with 3–5 coronal slices of each leg using Inveon Research Workshop (IRW) software. Regions of interest (ROI) were selected from PET images using

CT anatomical guidelines and the activity associated with them was measured with Inveon Research Workstation software (Siemens Medical Solutions, Knoxville, TN). Maximum standard uptake values (SUVs) for both experiments were calculated using SUV=([nCi/mL]x[animal weight (g)]/[injected dose (nCi)]). A post-PET biodistribution was carried out on the mice after the 24 h time point.

Statistical Analysis

All data are presented as mean±SD. To determine statistical significance, two-tailed unpaired t-tests were performed using GraphPad Prism, with $p < 0.05$ considered statistically significant.

RESULTS

Radiochemistry

Radiochemical purity of 96 ± 2% was achieved after 60 min at room temperature for ^{64}Cu-CB-TE1A1P-LLP2A with specific activity of 1 mCi/μg. At 40 °C, the reaction time was significantly reduced to 15 min, while at 90 °C, complete radiolabeling was achieved in 5 min(Figure 2). Under similar specific activity, radiochemical purity of ^{64}Cu-CB-TE2A-LLP2A was 68%± 3% after incubated at 90°C for 60 min No radiolabeling for CB-TE2A-LLP2A was observed under 40 °C after 60 min.

Cell binding Assays

Prior to the assays with the radiopharmaceutical, the B16F10 cells were analyzed for the surface expression of VLA-4 using flow cytometry (Figure 3A). B16F10 cells express high levels (>99%) of VLA-4 when normalized to the isotype control. The receptor-binding properties of ^{64}Cu-CB-TE1A1P-LLP2A were evaluated in B16F10 melanoma cell line by saturation binding assays performed at 4 °C. The binding affinity of ^{64}Cu-CB-TE1A1P-LLP2A was also investigated by determining the equilibrium dissociation constant (K_d) and the receptor concentration (B_{max}) of radiolabeled conjugate to B16F10 cells in a saturation binding assay. To demonstrate specific binding, a large excess of unlabeled LLP2A was added to cells to saturate the binding sites. A representative saturation binding curve of ^{64}Cu-CB-TE1A1P-LLP2A to B16F10 cells is shown in Figure 3. The data show that in the concentration range of 0.1–80 nM, ^{64}Cu-CB-TE1A1P-LLP2A is bound to a single class of binding sites with a K_d of 1.2±0.2 nM and a B_{max} of 471 ±14 fmol/mg, while ^{64}Cu-CB-TE2A-LLP2A has a K_d of 1.6 ±0.4 nM and B_{max} of 304 ± 18 fmol/mg.

Biodistribution of ^{64}Cu-CB-TE1A1P-LLP2A and ^{64}Cu-CB-TE2A-LLP2A in tumor bearing mice

^{64}Cu-CB-TE1A1P-LLP2A (14 μCi, 1000 μCi/μg)were injected into B16F10 tumor bearing C57BL/6 mice. The animals were sacrificed at 2 h post-injection, the organs of interest were harvested and the activity in each organ/tissue was measured. The data are compared to previously published data with ^{64}Cu-CB-TE2A-LLP2A.[10] The tumor and tissue uptake values are presented in Figure 4A. Liver uptake for both ^{64}Cu-labeled ligands is comparable (2.3 ± 0.3 %ID/g for ^{64}Cu-CB-TE1A1P-LLP2A and 2.4 ± 0.3 %ID/g for ^{64}Cu-CB-TE2A-LLP2A). Lower kidney uptake was observed for ^{64}Cu-CB-TE1A1P-LLP2A compared to ^{64}Cu-CB-TE2A-LLP2A (3.2 ±0.4 %ID/g vs. 4.7 ± 0.3 %ID/g, $p < 0.003$). ^{64}Cu-CB-TE1A1P-LLP2A exhibited higher uptake in the bone (6.2± 1.7 %ID/g) compared to ^{64}Cu-CB-TE2A-LLP2A (2.4± 0.4 %ID/g, $p < 0.01$). The tumor uptake for ^{64}Cu-CB-TE1A1P-LLP2A is significantly higher than ^{64}Cu-CB-TE2A-LLP2A (11.4 ± 2.3 %ID/g and 3.1± 0.6 %ID/g, respectively; $p < 0.001$). Higher uptake of ^{64}Cu-CB-TE1A1P-LLP2A compared to ^{64}Cu-CB-TE2A-LLP2A was also observed in other receptor abundant organs, including

spleen and marrow. Tracer uptake in the spleen was 17.9± 2.3 %ID/g for ^{64}Cu-CB-TE1A1P-LLP2A, which is significantly higher than 8.4± 2.1 %ID/g, for ^{64}Cu-CB-TE2A-LLP2A ($p \leq 0.001$). In addition, ^{64}Cu-CB-TE1A1P-LLP2A had higher uptake in marrow than ^{64}Cu-CB-TE2A-LLP2A(32.6 ± 19.0 %ID/g and 11.3± 2.6 %ID/g, respectively, $p < 0.03$). Tumor to blood ratios for ^{64}Cu-CB-TE1A1P-LLP2A and ^{64}Cu-CB-TE2A-LLP2A are 19.5 ± 3.0 and 4.2 ± 1.4, respectively ($p < 0.001$) (Figure 4B). Similarly, the tumor to muscle ratio for ^{64}Cu-CB-TE1A1P-LLP2A was significantly higher than for ^{64}Cu-CB-TE2A-LLP2A at 2 h (^{64}Cu-CB-TE1A1P-LLP2A = 13.0 ± 1.4, ^{64}Cu-CB-TE2A-LLP2A = 5.5 ± 0.9, $p < 0.001$). As shown in Figure 4C, in a separate blocking study, ^{64}Cu-CB-TE1A1P-LLP2A was co-administered with cold (non-radioactive) excess LLP2A ligand. In the presence of the blocking agent, the radiotracer uptake was significantly reduced in the tumor, spleen and bone, demonstrating the targeting specificity of ^{64}Cu-CB-TE1A1P-LLP2A to $\alpha_4\beta_1$ receptors in these tissues.

Small animal PET/CT images

Figure 5A shows the small animal PET/CT imaging of B16F10 tumor-bearing mice 2 h and 24 h after injection of ^{64}Cu-CB-TE1A1P-LLP2A and ^{64}Cu-CB-TE2A-LLP2A. Uptake in the tumor was clearly visible at 2 h and the co-injection of cold LLP2A resulted in significant decreased signal. The decreased uptake was observed after 24 h for two compounds. Figure 5B shows the tumor to background ratios calculated based on SUVs from imaging data at 2 and 24 h in tumor-bearing mice. ^{64}Cu-CB-TE1A1P-LLP2A had a more than 2-fold higher tumor to background ratio than ^{64}Cu-CB-TE2A-LLP2A (17.5 ±1.6 and 7.4± 0.5, respectively; p = 0.0001). With the blocking, the tumor to background ratio were significantly reduced to 8.2 ± 0.8 for ^{64}Cu-CB-TE1A1P-LLP2A ($p < 0.005$) and 4.2 ± 0.3 for ^{64}Cu-CB-TE2A-LLP2A ($p<0.01$). After 24h, the tumor to background ratios for ^{64}Cu-CB-TE1A1P-LLP2A and ^{64}Cu-CB-TE2A-LLP2A decreased to 9.0± 0.4 and 5.1 ± 0.4, respectively.

DISCUSSION

Integrin $\alpha_4\beta_1$ plays an important role in the regulation of immune cell recruitment to inflamed endothelium and sites of inflammation.[16] It is a promising diagnostic target found in leukemias, lymphomas, melanomas and sarcomas.[3,17,18] It has been reported that malignant melanomas demonstrated an increase in the expression of $\alpha_4\beta_1$ compared with benign melanocytic lesions.[19] Integrin $\alpha_4\beta_1$ also participates in cell-lymphocyte interactions, retention and migration of immature progenitors in the bone marrow, and is involved in cancer cell trafficking, metastasis and other events.[19–22] Thus, it would be highly desirable to have a sensitive, non-invasive imaging probe for $\alpha_4\beta_1$ positive tumors, as well as for imaging bone marrow-derived cell types.

A new class of cross-bridged cyclam-based macrocycles featuring phosphonate pendant arms was recently developed. CB-TE1A1P had been shown to readily form a neutral copper(II) complex at room temperature with specific activity > 1 mCi/μg. Biodistribution studies demonstrated that ^{64}Cu-CB-TE1A1P rapidly cleared the circulation with similar accumulation in non-target organs/tissues when compared ^{64}Cu-labeled CB-TE2A.

Previously, small animal PET imaging of ^{64}Cu-CB-TE2A-LLP2A showed excellent targeting in the Raji lymphoma mouse model.[9] A following study also demonstrated that ^{64}Cu-CB-TE2A-LLP2A could visualize bone marrow derived cells implicated in the pre-metastatic niche.[10] In this study, we report the *in vitro* and *in vivo* behavior of ^{64}Cu-CB-TE1A1P-LLP2A compared to ^{64}Cu-CB-TE2A-LLP2A, demonstrating the important effect of chelator on receptor targeting and non-target tissue clearance.

CB-TE1A1P-LLP2A chelated ^{64}Cu at 90 °C for only 5 min compared to 60 min for CB-TE2A-LLP2A using the same labeling buffer (0.1 M NH_4OAc, pH 8.1). After further optimization, higher specific activity for ^{64}Cu-CB-TE1A1P-LLP2A (> 1 mCi/μg) was achieved compared to ^{64}Cu-CB-TE2A-LLP2A (typically 300–500 μCi/μg). It was also found that CB-TE1A1P-LLP2A can be labeled with ^{64}Cu at room temperature after 60 min, although this is somewhat longer than ^{64}Cu-labeling of the chelator CB-TE1A1P alone (30 min). We conclude that after conjugation of the carboxymethyl pendant arm to LLP2A via a hydrophilic linker, the kinetics of CB-TE1A1P complexation to copper at room temperature is some what slower. However, the somatostatin receptor targeted conjugate CB-TE1A1P-Y3-TATE only achieved about 60% radiolabeling at room temperature at 60 min, indicating that the hydrophilic linker between CB-TE1A1P and LLP2A enables faster kinetics than direct conjugation of the carboxylate of CB-TE1A1P and the N-terminal amine on Y3-TATE.[23]

Flow cytometery using a-4 specific antibody confirmed high VLA-4 expression on B16F10 cells (>99%) as compared to the isotype control (Figure 3A). Comparable *in vitro* binding affinities for $\alpha_4\beta_1$ integrin receptors from B16F10 cells were determined for ^{64}Cu-CB-TE1A1P-LLP2A and ^{64}Cu-CB-TE2A-LLP2A; however, the receptor concentration (B_{max})for ^{64}Cu-CB-TE1A1P-LLP2A (471 fmol/mg) was significantly greater than for ^{64}Cu-CB-TE2A-LLP2A(304 fmol/mg; $p < 0.03$), suggesting that the CB-TE1A1P chelator enables LLP2A binding to more receptors. The increase in B_{max} may be due to the minor structural alteration and stabilization of the Cu(II)-CB-TE1A1P chelate in the lipid-rich environment of the receptor.

In the biodistribution studies, comparable mass amounts of ^{64}Cu-CB-TE1A1P-LLP2A (14 μCi, 14 ng)and ^{64}Cu-CB-TE2A-LLP2A (5μCi, 12.5 ng) were administrated per mouse. Higher uptake in $\alpha_4\beta_1$ rich organs were observed for ^{64}Cu-CB-TE1A1P-LLP2A than for ^{64}Cu-CB-TE2A-LLP2A at 2 h post-injection, indicating superior targeting properties of ^{64}Cu-CB-TE1A1P-LLP2A. These data demonstrate that the ^{64}Cu-chelate has a significant impact on the target tissue uptake of the targeting ligand, in this case, LLP2A. In a previous study comparing the CB-TE2A and CB-TE1A1P chelators with the somatostatin agonist, Y3-TATE, a significant but not dramatic improvement in targeting and non-target tissue uptake was observed with the CB-TE1A1P conjugate.[23] We observed 2–3-fold increases in target tissue (tumor, spleen, bone marrow) uptake with the CB-TE1A1P- vs the CB-TE2A-LLP2A conjugate, and tumor: blood and tumor: muscle ratios were 2–4-fold higher.

Comparable accumulation in the liver was observed for ^{64}Cu-CB-TE1A1P-LLP2A and ^{64}Cu-CB-TE2A-LLP2A. However, increased kidney uptake was found in ^{64}Cu-CB-TE2A-LLP2A compared to ^{64}Cu-CB-TE1A1P-LLP2A. Considering the net charge of 0 for ^{64}Cu-CB-TE2A-LLP2A and -1 for ^{64}Cu-CB-TE1A1P-LLP2A, the result is consistent with previous studies that the addition of negative charges to peptide conjugates reduces renal radioactivity levels.[24–25]

Small animal PET/CT images of ^{64}Cu-CB-TE1A1P-LLP2A and ^{64}Cu-CB-TE2A-LLP2A showed that tumors can be clearly visualized with better contrast than was observed for ^{64}Cu-CB-TE1A1P-LLP2A. Quantification of the activity in tissues indicated that ^{64}Cu-CB-TE1A1P-LLP2A had improved tumor to background ratios compared with ^{64}Cu-CB-TE2A-LLP2A, consistent with the biodistribution study and demonstrating that ^{64}Cu-CB-TE1A1P-LLP2A is a promising probe for imaging $\alpha_4\beta_1$ positive tumors.

CONCLUSION

The bifunctional chelator CB-TE1A1P was successfully conjugated with LLP2A, a high-affinity peptidomimetic ligand against $\alpha_4\beta_1$ integrin. *In vivo* evaluation shows that ^{64}Cu-CB-TE1A1P-LLP2A had dramatically improved tumor-to-background contrast compared with ^{64}Cu-CB-TE2A-LLP2A. ^{64}Cu-CB-TE1A1P-LLP2A will serve as an excellent PET radiopharmaceutical for the imaging of $\alpha_4\beta_1$ positive tumors, which include lymphoma, melanoma and multiple myeloma, and this agent has potential for improved imaging of bone marrow derived cells of the pre-metastatic niche.

Supplementary Material

Refer to Web version on PubMed Central for supplementary material.

Acknowledgments

The authors gratefully acknowledge Chris Sherman, Jalpa Modi, Michael Zahner, Margaret Morris and Nicole Fettig for technical support and Julie Schwarz, MD, PhD for helpful discussions. This research was supported by NIH/NCI 5 R01 CA 093375 (CJA) and DOE DE-FG02-08ER64671 (Integrated Research Training Program of Excellence in Radiochemistry awarded to Michael J. Welch for partial support to MJ).

References

1. Hynes RO. Integrins: bidirectional, allosteric signaling machines. Cell. 2002; 110:673–677. [PubMed: 12297042]
2. Gupta MK, Qin R. Mechanism and its regulation of tumor-induced angiogenesis. World J Gastroenterol. 2003; 9:1144–1155. [PubMed: 12800214]
3. Holzmann B, Gosslar U, Bittner M. α_4 integrins and tumor metastasis. Curr Top Microbiol Immunol. 1998; 231:125–141. [PubMed: 9479864]
4. de la Fuente MT, Casanova B, Garcia-Gila M, Silva A, Garcia-Pardo A. Fibronectin interaction with $\alpha_4\beta_1$ integrin prevents apoptosis in B cell chronic lymphocytic leukemia: correlation with Bcl-2 and Bax. Leukemia. 1999; 13:266–274. [PubMed: 10025901]
5. Hsia DA, Lim ST, Bernard-Trifilo JA, Mitra SK, Tanaka S, Hertog JD, Streblow DN, Ilic D, Ginsberg MH, Schlaepfer DD. Integrin $\alpha_4\beta_1$ promotes focal adhesion kinase-independent cell motility via α_4 cytoplasmic domain-specific activation of c-Src. Mol Cell Biol. 2005; 25:9700–9712. [PubMed: 16227616]
6. Fischman AJ, Babich JW, Strauss HW. A ticket to ride: peptide radiopharmaceuticals. J Nucl Med. 1993; 34:2253–2263. [PubMed: 8254420]
7. Okarvi SM. Peptide-based radiopharmaceuticals: future tools for diagnostic imaging of cancers and other diseases. Med Res Rev. 2004; 24:357–397. [PubMed: 14994368]
8. Peng L, Liu R, Marik J, Wang X, Takada Y, Lam KS. Combinatorial chemistry identifies high-affinity peptidomimetics against $\alpha_4\beta_1$ integrin for *in vivo* tumor imaging. Nat Chem Biol. 2006; 2:381–389. [PubMed: 16767086]
9. DeNardo SJ, Liu R, Albrecht H, Natarajan A, Sutcliffe JL, Anderson CJ, Peng L, Ferdani R, Cherry SR, Lam KS. ^{111}In-LLP2A-DOTA polyethylene glycol-targeting $\alpha_4\beta_1$ integrin: comparative pharmacokinetics for imaging and therapy of lymphoid malignancies. J Nucl Med. 2009; 50:625–634. [PubMed: 19289419]
10. Shokeen M, Zheleznyak A, Wilson JM, Jiang M, Liu R, Ferdani R, Lam KS, Schwarz JK, Anderson CJ. Molecular imaging of very late antigen-4 ($\alpha_4\beta_1$ integrin) in the premetastatic niche. J Nucl Med. 2012; 53:1–8. [PubMed: 22159159]
11. Sprague JE, Peng Y, Sun X, Weisman GR, Wong EH, Achilefu S, Anderson CJ. Preparation and biological evaluation of copper-64-labeled tyr3-octreotate using a cross-bridged macrocyclicchelator. Clin Cancer Res. 2004; 10:8674–8682. [PubMed: 15623652]

12. Boswell CA, Sun X, Niu W, Weisman GR, Wong EH, Rheingold AL, Anderson CJ. Comparative in vivo stability of copper-64-labeled cross-bridged and conventional tetraazamacrocyclic complexes. J Med Chem. 2004; 47:1465–1474. [PubMed: 14998334]

13. Stigers DJ, Ferdani R, Weisman GR, Wong EH, Anderson CJ, Golen JA, Moore C, Rheingold AL. A new phosphonatependant-armed cross-bridged tetraaminechelator accelerates copper (ii) binding for radiopharmaceutical applications. Dalton Trans. 2010; 39:1699–1701. [PubMed: 20449406]

14. Ferdani R, Stigers DJ, Fiamengo AL, Wei LBT, Golen JA, Rheingold AL, Weisman GR, Wong EH, Anderson CJ. Synthesis, Cu(ii) complexation, ^{64}Cu-labeling and biological evaluation of cross-bridged cyclamchelators with phosphonate pendant arms. Dalton Trans. 2012; 41:1938–1950. [PubMed: 22170043]

15. Weisman GR, Rogers ME, Wong EH, Jasinski JP, Paight ES. Cross-bridged cyclam: protonation and Li+ complexation in a diamond-lattice cleft. J Am Chem Soc. 1990; 112:8604–8605.

16. Luster AD, Alon R, Andrian UH. Immune cell migration in inflammation: present and future therapeutic targets. Nature Immunology. 2005; 6:1182–1190. [PubMed: 16369557]

17. Miyake K, Hasunuma Y, Yagita H, Kimoto M. Requirement for VLA-4 and VLA-5 integrins in lymphoma cells binding to and migration beneath stromal cells in culture. J Cell Biol. 1992; 119:653–662. [PubMed: 1400595]

18. Juneja HS, Schmalsteig FC, Lee S, Chen J. Vascular cell adhesion molecule-1 and VLA-4 are obligatory adhesion proteins in the heterotypic adherence betwenn human leukemia/lymphoma cells and marrow stromal cells. Exp Hematol. 1993; 21:444–450. [PubMed: 7680000]

19. Schadendorf D, Gawlik C, Haney U, Ostmeier H, Suter L, Czarnetzki BM. Tumour progression and metastatic behaviour in vivo correlates with integrin expression on melanocytic tumours. J Pathol. 1993; 170:429–434. [PubMed: 8105045]

20. Yoneda T. Cellular and molecular basis of preferential metastasis of breast cancer to bone. J Orthop Sci. 2000; 5:75–81. [PubMed: 10664443]

21. Lapidot T, Dar A, Kollet O. How do stem cells find their way home? Blood. 2005; 106:1901–1910. [PubMed: 15890683]

22. Kuphal S, Bauer R, Bosserhoff AK. Integrin signaling in malignant melanoma. Cancer Metastasis Rev. 2005; 24:195–222. [PubMed: 15986132]

23. Guo Y, Ferdani R, Anderson CJ. Preparation and biological evaluation of 64Cu labeled Tyr^3-Octreotate using a phosphonic acid-based cross-bridged macrocyclic chelator. Bioconjugate Chem. 2012; 23:1470–1477.

24. Jones-Wilson TM, Deal KA, Anderson CJ, McCarthy DW, Kovacs Z, Motekaitis RJ, Sherry AD, Martell AE, Welch MJ. The in vivo behavior of copper-64-labeled azamacrocyclic complexes. Nucl Med Biol. 1998; 25:523–530. [PubMed: 9751418]

25. Akizawa H, Arano Y, Mifune M, Iwado A, Saito Y, Mukai T, Uehara T, Ono M, Fujioka Y, Ogawa K, Kiso Y, Saji H. Effect of molecular charges on renal uptake of ^{111}In-DTPA-conjugated peptides. Nucl Med Biol. 2001; 28:761–768. [PubMed: 11578896]

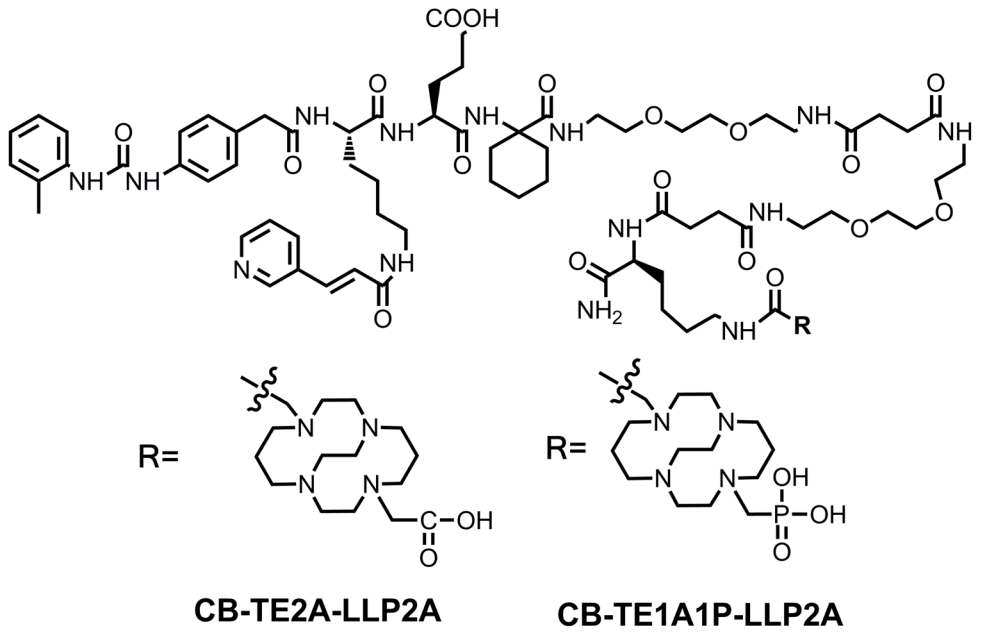

Figure 1.
Structure of CB-TE1A1P-LLP2A and CB-TE2A-LLP2A.

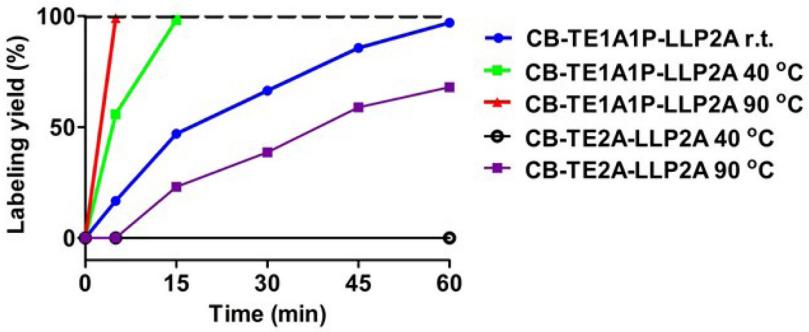

Figure 2.

Radiolabeling yields of CB-TE1A1P-LLP2A and CB-TE2A-LLP2A with ^{64}Cu in 0.1 M NH_4OAc (pH 8.0) at different temperatures. The specific activity is 1 mCi/μg.

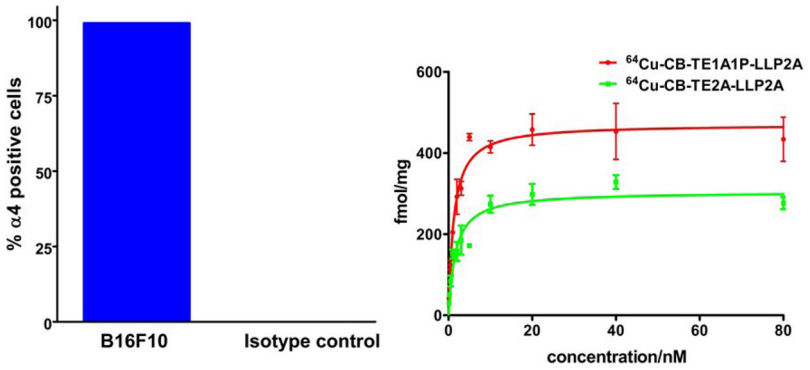

Figure 3.

Percentage of α_4(VLA-4)positive cells in total B16F10 tumor cell population as determined by flow cytometry (Anti-Mouse CD49d (integrin a-4) (eBioscience). Greater than 99% cells were positive for VLA-4 (A). The binding of ^{64}Cu-CB-TE1A1P-LLP2A and ^{64}Cu-CB-TE2A-LLP2A to integrin $\alpha_4\beta_1$ was determined by a saturation binding assay in B16F10 melanoma cells (n=3 for each data point; mean value ± SE). The K_d for ^{64}Cu-CB-TE1A1P-LLP2A and ^{64}Cu-CB-TE2A-LLP2A are 1.2 ± 0.2 nM and 1.6 ± 0.4 nM, respectively. The receptor concentrations (B_{max}) for ^{64}Cu-CB-TE1A1P-LLP2A and ^{64}Cu-CB-TE2A-LLP2A are 471 ± 14 and 304 ± 18 fmol/mg, respectively ($p < 0.03$).

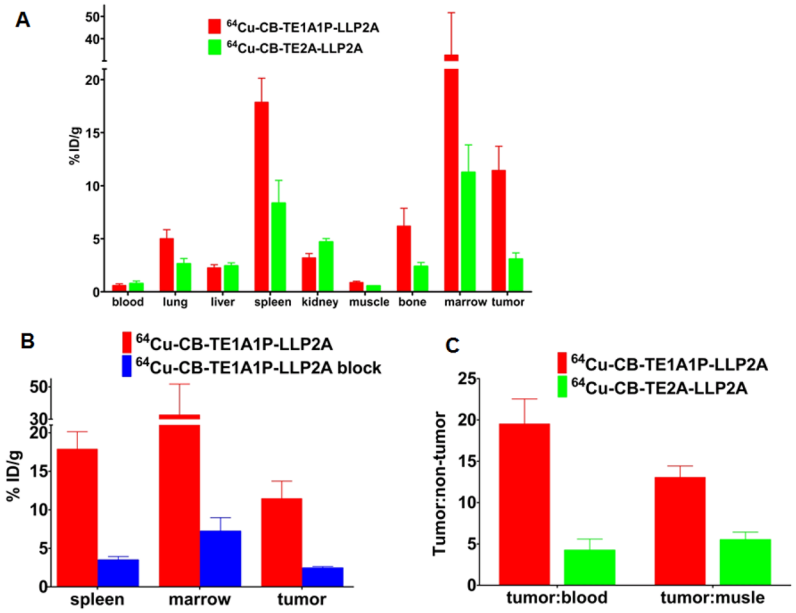

Figure 4.

Biodistribution in selected organs 2 h post-injection of ^{64}Cu-CB-TE1A1P-LLP2A (14 μCi, 14 ng) and ^{64}Cu-CB-TE2A-LLP2A (5 μCi, 12.5 ng) in B16F10 tumor-bearing mice (A). Comparison of tumor: blood and tumor: muscle ratios of ^{64}Cu-CB-TE1A1P-LLP2A and ^{64}Cu-CB-TE2A-LLP2A (B). A blocking study shows specific binding for ^{64}Cu-CB-TE1A1P-LLP2A (n=3–5 for each data point; bars ± SE) (C).

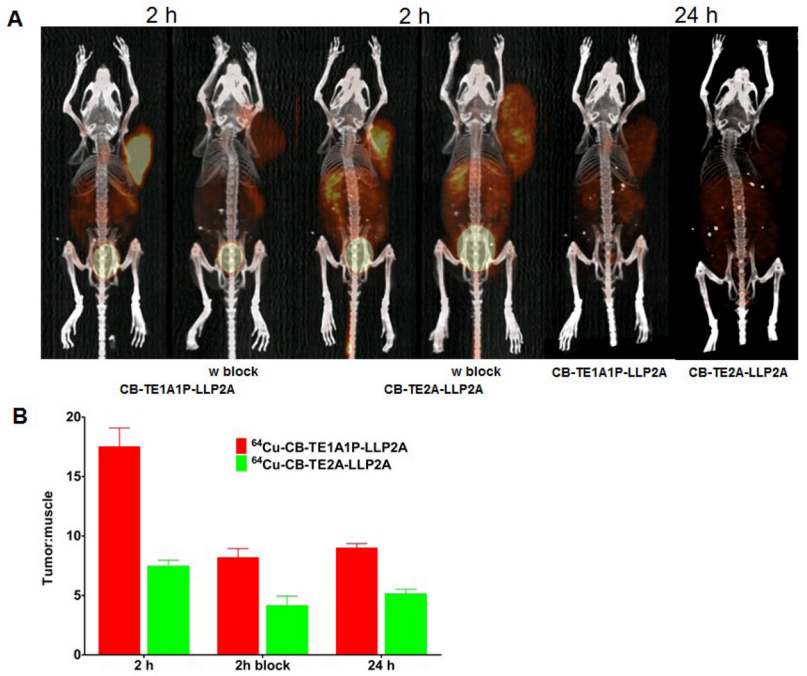

Figure 5.

Small-animal PET/CT imaging of B16F10 tumor-bearing mice at 2 h, with or without coinjection of excess amount of LLP2A and 24 h post-injection of ^{64}Cu-CB-TE1A1P-LLP2A (100 μCi; 0.67 μg) and ^{64}Cu-CB-TE2A-LLP2A (100 μCi; 0.67 μg) (A). The Tumor: background ratios at 2 and 24h were calculated from the MIP images (SUVs) of tumor-bearing C57BL/6 mice (n = 2; bars ± SE) (B).